Evaporative Mist Cooling as Heat Dissipation Technique: Experimental Assessment and Modelling

MCarmen Guerrero Delgado [1], José Sánchez Ramos [2] , Servando Álvarez Domínguez [1], Francisco Toral Ulloa [3] and José Antonio Tenorio Ríos [3],*

[1] Grupo de Termotecnia, Escuela Superior de Ingenieros, Universidad de Sevilla, Camino de los Descubrimientos s/n, 41092 Sevilla, Spain; mgdelgado@us.es (M.G.D.); salvarez@us.es (S.Á.D.)

[2] Máquinas y Motores Térmicos, Escuela Superior de Ingeniería, Av. Universidad de Cádiz, 10, 11519 Puerto Real, Spain; jsr@us.es

[3] Instituto de Ciencias de la Construcción Eduardo Torroja-CSIC, Serrano Galvache 4, 28033 Madrid, Spain; francisco.toral@ietcc.csic.es

* Correspondence: tenorio@ietcc.csic.es

Abstract: The severity of extreme weather conditions brought on by climate change are conditioning quality of life, economic development, and well-being in today's cities. Conventional measures have been shown to be insufficient for tackling climate change and must be supplemented with ecofriendly approaches. Hence, the scientific community's endeavor to develop natural cooling techniques that lower energy consumption while delivering satisfactory comfort levels. For its simplicity and low cost, evaporative cooling has gained in popularity in recent years. The substantial cooling power to be drawn from evaporative mist cooling, makes it an attractive alternative to conventional systems. Research conducted to date on the technique has focused on producing cold air, whilst cooling the water involved has been neither assessed nor experimentally validated. No readily applicable simplified model for the system able to use operating parameters as input variables has been defined either. The present study consequently aimed to experimentally assess the cooling power of the evaporation of sprayed water and experimentally validate a simplified model to assess and design such systems. The findings confirmed the cooling power of the technique, with declines in water temperature of up to 6 °C, and with it the promise afforded by this natural air conditioning method. Finally, simplified model developed allows to evaluate this technique like a conventional system for producing fresh water.

Keywords: mitigation technologies; natural sinks; passive cooling; heat dissipation

1. Introduction

1.1. Context

The ever greater climate change that is of such concern today, in conjunction with population growth and economic development, has had a severe impact on air conditioning-related energy consumption [1]. Recent studies have shown that if temperatures rise as predicted, worldwide residential energy consumption for cooling will be up to 34% higher than at present in 2050 and 2100 up to 61% greater [2], except in the Mediterranean area where a still higher value may be expected [3]. Even today, severely warm temperatures in city centers [4] limit the use of urban areas in the summer months. The aforementioned cooling techniques could condition semi-enclosed spaces to adapt cities to the new conditions imposed by climate change and favor a return to outdoor living [5]. These circumstances generate a need to use passive natural techniques to reduce energy consumption

and protect the environment while delivering satisfactory comfort levels [6,7]. A wide spectrum of natural and passive techniques are presently in places, such as solar control systems, excess heat dissipation into natural low temperature (air, water, and soil) heat sinks and the use of a building's thermal mass to absorb excess heat [8]. The significant cooling power to be found in natural techniques could lower cooling-induced energy demand considerably [9]. Their performance depends largely on climate [6]; however, they may prove insufficient to meet indoor comfort requirements, although such facilities may serve as pre-conditioning systems in interiors. This study explores the use of natural and passive techniques as alternative approaches to cooling semi-enclosed spaces.

1.2. Passive Natural Cooling Techniques

Urban buildings and spaces exchange energy with the surrounding environment naturally, dissipating heat to lower temperature media. Dissipation techniques are applicable where heat gain can be lowered with the aid of a suitable exchange medium. The elements involved in that natural mechanism are the sky, air, water, and soil, all of which act as sinks.

Given the suitability of its thermal properties, water, deemed a bioclimatic vehicle for conditioning outdoor spaces, is the most commonly used fluid heat carrier. The abundance of water on the planet has favored its use in cooling for centuries. It is applied as a dissipation fluid in systems where heat is released across conventional elements such as fan coils [10–12] or radiators [13–15], as well as in innovative approaches such as thermally activated building systems (TABS) [16,17]. The need to cool urban heat islands, in conjunction with the planet's present energy dilemma, posit the use of natural techniques to generate low temperature water by capitalizing on soil temperatures [18–20], nightly radiant cooling [21–25], and evaporative cooling systems [26–29].

The potential of water-based systems to mitigate heat stress has been explored in depth by authors analyzing temperature patterns in cities surrounded by bodies of water. Urban wetlands contribute to "urban cool islands" where temperatures may be 1 °C to 2 °C lower than in other areas [30]. In addition to natural bodies of water in cities, many evaporative elements such as ponds and fountains have been used for cooling as well as decorative purposes [31,32].

1.3. Evaporative Cooling

This study focused on the use of evaporative systems as a natural cooling technique. Evaporative cooling begins when unsaturated air comes into contact with drops of water. The underlying principle is based on the absorption of atmospheric heat by the water until it evaporates; thereby, lowering system temperature.

In open or semi-enclosed urban spaces, the most prominent evaporative cooling systems are ponds and mists. Evaporative cooling system efficiency is greater where the air-water contact area is large or when the water flows and disperses, as in fountains or mists [31].

The atomizing or misting nozzle is the element that converts water flow into hosts of small particles varying in diameter and mass. Droplet scatter increases the air-water contact area and with it evaporative mist cooling efficiency, which depends largely on nozzle type, droplet diameter, and local climate [33–35].

A review of the literature reveals that to date research has targeted cold air production [36–38], whereas production of the cold water involved has been neither assessed nor experimentally validated. As cooling the water mass narrows, the gap between energy production and use, optimizing evaporation, it is an issue worth exploring.

1.4. Aims

Simplicity, low cost, and use of renewable resources are the factors behind the growing popularity of evaporative cooling. The substantial cooling power that makes evaporative mist cooling an attractive alternative to conventional systems informed this study.

The research conducted on the technique to date has focused on cold air production, whilst no assessments or experimental testing have been conducted on the cold water production involved. Neither has the scientific community developed simplified models using operating parameters as input variables to enhance their applicability.

The present study consequently aimed to empirically assess the cooling power of evaporative mist cooling and experimentally validate a simplified model to assess and design such systems.

2. Experimental Set-Up

2.1. Overview

The methodology deployed in pursuit of the aims set out in Section 1.4 was essentially empirical to assess natural cooling and develop a simplified model for the system. The starting point for that methodology was an experimental analysis of dissipation system behavior.

The effect of cooling a mass of water with different evaporative techniques entailed the use of two identical ponds, only one of which was fitted with sprayers. The reference was the pond not so fitted. Both were monitored continually, and their cooling performance subsequently assessed. In addition to assessing the cooling power attributable to their presence, two types of high performance nozzles were used to manufacturer instructions and their efficiency compared.

The experimental assessment was taken as a basis for quantifying the power of the cooling technique and the development of a calibrated simplified model informed by empirical reality. The input variables consisted in system physical magnitudes as listed in manufacturers' datasheets.

2.2. Experimental Design

The experimental setup described above is illustrated in Figure 1. The 1 m³ concrete experimental and reference ponds were lined with 5 cm thick insulation to minimize thermal loss.
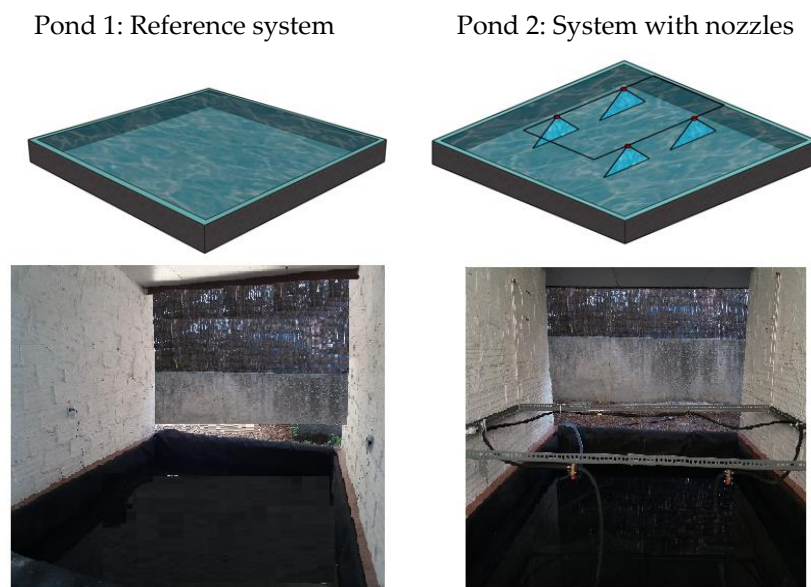
Pond 1: Reference system   Pond 2: System with nozzles

Figure 1. Experimental and reference ponds.

The flat fan nozzles used delivered a flow of 1 L/min to 3 L/min, depending on the working pressure. Two models were analyzed, HARDI ISO F-110-04 (red) and HARDI ISO F-110-06 (grey). The sprayers were spaced in pond 2 far enough apart to ensure they did not interfere with standard operation. Their distribution in the pond, shown in Figure 2, was determined bearing in mind each device's spray diameter.
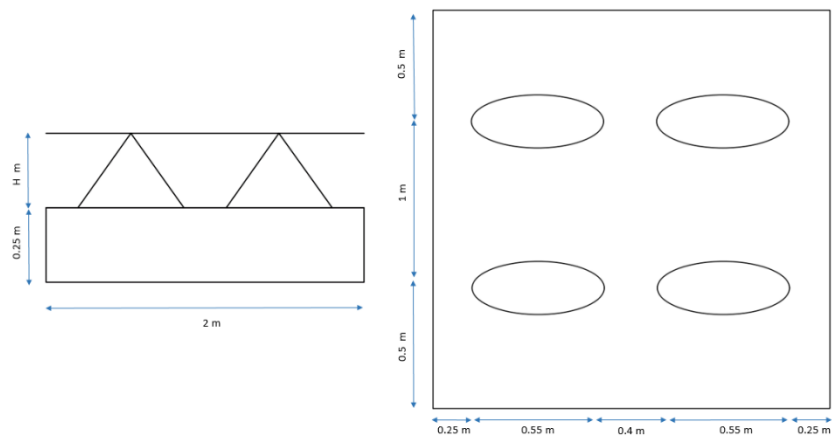
Figure 2. Sprayer distribution in pond 2.

A water heater ensured the water was at the same temperature in the two ponds at start-up and two pumps, one for each, mixed the water when the cooling system was idle. One of the pumps is used to generate the sprays in the nozzles. This pump drives a small flow at variable pressure. The nominal power is 600 W. On the other hand, the other pump is a circulation pump, its usefulness is to guarantee that at the beginning of the experiment the temperature of both ponds is the same by mixing both. The electric power is 200 W.

This dissipation technology is the combination of pond and sprayers. The cost of the nozzles is between 3–4 €/unit. However, the main cost is due to the construction of the pond and the pump system. Total cost for this system is dependent on the application.

2.3. Monitoring System

The monitoring system was designed to compile data on the variables used to assess system parameters and energy consumption: water temperature in the two ponds, amount of water evaporated, and outdoor air conditions (outdoor wet and dry bulb temperature and relative humidity).

2.3.1. Pond Water Temperature

The water temperature in the two ponds to be cooled was monitored with type T thermocouples operating in the −200 °C to +260 °C range at a precision of ±0.1 °C. These sensors, consisting in one copper alloy and one copper-nickel (55%/45%) wire, were calibrated with a Fluke Calibration 9142 instrument designed to cool to −25 °C and heat to +660 °C with a precision of ±0.01 °C. The thermocouples, which measured the water temperature directly, were positioned at different points and heights in the ponds (see Figure 3).
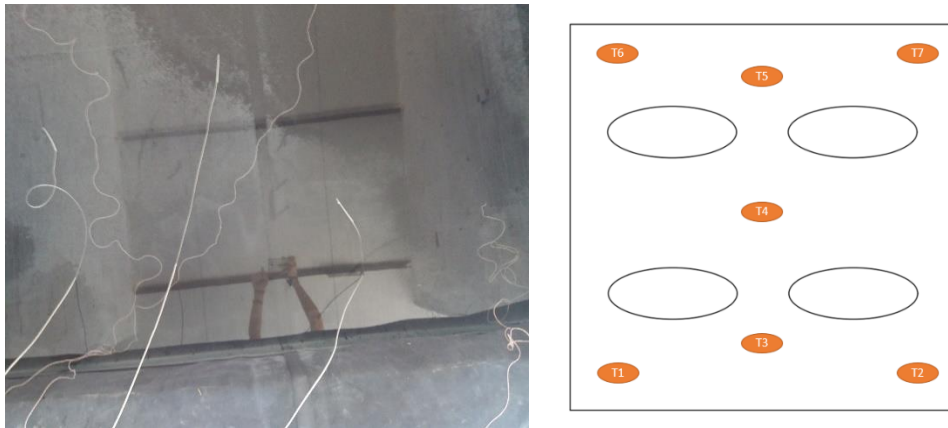
Figure 3. Sensor positions in ponds.

2.3.2. Evaporation Measurement

Another parameter essential to system characterization was the amount of water evaporating out of the ponds, whose containers were graduated for that purpose (see Figure 4). The water level shown at any given time was used to find the percentage of water evaporating as a result of the evaporative cooling-mediated decline in pond water temperature.

Figure 4. Measurement of volume of evaporated water.

2.3.3. Outdoor Weather

Outdoor temperature, wind velocity, and relative humidity values were obtained at 1 min intervals from a weather station near the site of the experiment with a precision of ±0.1% for temperature and wind velocity and ±1% for relative humidity. In addition, local sensors have been installed in situ to verify and duplicate the measurements from the weather station. They are Elitech RC-4HC outdoor air temperature-relative humidity sensors with a measuring range of −30 °C to +60 °C for T and 0% to 99% for relative humidity. The precision for temperature was ±0.1% and for relative humidity ±1%. Similarly, since wind speed is a very local variable, a PCE-ADL 11 anemometer was installed in the vicinity of the prototype. The operating range varies from 1–30 m/s, with a resolution of ±0.01. As wind velocity is a very local variable, a PCE-ADL 11 anemometer operating at 1 m/s to 30 m/s with a resolution of ±0.01 was positioned in the vicinity of the prototype.

2.4. Testing

The tests conducted were designed to experimentally assess the cooling power of evaporative mist cooling and experimentally develop and validate a simplified model to assess and design such systems.

They can be classified by the aim pursued:

- Experiment 1: assessment of thermal loss in the ponds.
- Experiment 2: analysis of cooling power and the development, calibration, and validation of the simplified model proposed.
- Experiment 3: analysis of the sensitivity of the proposed simplified model parameters.

The aforementioned experiments were conducted in the consecutive order shown in Table 1, for each depending on the findings of its predecessors.

2.4.1. Experiment 1

To assess their thermal loss, pond behaviour was analysed with the sprayers off. One of the aims pursued in this study was to compare the cooling power of misting to the power of unaided evaporation in the same volume of water exposed to the air. Thermal loss in the absence of sprayer activity in the two ponds when exposed to the same environmental conditions consequently had to be identical to ensure the effect of misting was reliably measured.

2.4.2. Experiment 2

To meet the aims of this experiment set out in Section 2.4, the misting system described above was turned on for 8 h overnight (when wet bulb temperature was lowest), jetting the water down from a height of 0.5 m at a standard pressure of 2 bar. Further to the datasheets for the nozzles analysed [39] at that pressure, the operating flow was 1.31 L/min for HARDI ISO F-1110-04 and 1.06 L/min for HARDI F-110-06. Bar 2 pressure was chosen because it is the standard pressure in water supply systems, whilst 0.5 m was the manufacturer-recommended height to minimize airflow-induced drift loss.

2.4.3. Experiment 3

The parameters for the simplified model proposed in Section 4, whose variation was the objective sought in experiment 3, were nozzle height and pressure, the only two independent variables associated with system operation.

Any change in height has a significant impact on cooling, for it modifies droplet travel. At the greater height, the contact time between air and droplet is longer and more energy is exchanged. To assess that impact experimentally, pond evaporation was also monitored with the nozzles at 0.2 m, 0.4 m, and 0.6 m (heights relative to the water surface).

Similarly, according to manufacturer specifications, flow is determined by the working pressure [39], which may vary from 2 bar to 5 bar. Therefore, in addition to using the standard 2 bar pressure, the experiment was run at 3 bar and 5 bar, as quantified with the manometer built into the pump supplied with the sprayers.

2.4.4. Experimental Programme

The tests described above were conducted over 5 weeks period in September–October 2019, as shown in Table 1. Experiment 1, designed to characterize and validate thermal losses in the two ponds, was run during the first week. In experiment 2, conducted in weeks 2 and 3, the cooling power of misting was compared to cooling induced by unaided evaporation in a pond open to the air. The effect of the two modifiable variables associated with system operation on cooling efficiency was determined in weeks 4 and 5.

Table 1. Experimental plan.

	Day 1	Day 2	Day 3	Day 4	Day 5	Day 6	Day 7
Week 1	**Experiment 1**						
	Two ponds without misting facility						
Week 2	**Experiment 2**						
	HARDI ISO F-110-04 Height: 0.5 m Pressure: 2 bar						
Week 3	**Experiment 3**						
	HARDI ISO F-110-04 Height: 0.5 m Pressure: 2 bar						
Week 4	**Experiment 4**						
	HARDI ISO F-110-04 Height: 0.2 m Pressure: 2 bar	HARDI ISO F-110-04 Height: 0.4 m Pressure: 2 bar	HARDI ISO F-110-04 Height: 0.6 m Pressure: 2 bar	HARDI ISO F-110-04 Height: 0.5 m Pressure: 3 bar	HARDI ISO F-110-04 Height: 0.5 m Pressure: 4 bar	HARDI ISO F-110-04 Height: 0.5 m Pressure: 5 bar	HARDI ISO F-110-06 Height: 0.5 m Pressure: 2 bar
Week 5	**Experiment 4**						
	HARDI ISO F-110-06 Height: 0.4 m Pressure: 2 bar	HARDI ISO F-110-06 Height: 0.6 m Pressure: 2 bar	HARDI ISO F-110-06 Height: 0.5 m Pressure: 3 bar	HARDI ISO F-110-06 Height: 0.5 m Pressure: 4 bar	HARDI ISO F-110-06 Height: 0.5 m Pressure: 5 bar		

3. Natural Cooling Technique Modelling

3.1. Theoretical Fundamentals

General models attempt to determine the effect of changes in meteorological variables, system geometry and functional conditions on the temperature of a body of water. The model proposed is based on the behaviour of a single droplet inflowing air. Its main assumptions are the behaviour of the spray is related to the behaviour of a single droplet and the environment is not modified by movement of the droplet, nor the transfer of heat and mass from the drop. These hypotheses are not a limitation for the work since the aim is to know the functional dependence of the cooling efficiency on the water pond. Conservation equations of mass, energy, and momentum are used with the following assumptions [40]: the water drop is considered to be a sphere; there are no interactions among different water drops; the whole volume of the water drop is at the same temperature; and air temperature and pressure remain constant for each water drop and negligible radiant heat fluxes.

The parameters of greatest interest to determine the behaviour of that droplet are its radius and temperature, whose values can be found by solving a system of four equations, the conservation of momentum (Equations (1) and (2)), energy balance (Equation (4)) and conservation of mass (Equation (5)), that define the detailed model for a single droplet inflowing air [41].

The equations for conservation of momentum in the droplet are obtained using the second law of Newton (Equations (1) and (2)). Equations (1) and (3) are based on the forces acting on it: gravity, buoyancy, and friction, which govern its entire trajectory. Terminal velocity of a particle falling in gas is determined by the balance of friction force in Newtonian form and it is acting the projection of the particle surface area by friction, the buoyancy of the particle in gas, and the force making the particle fall. So, the friction force has x and y components.

$$\frac{dv_x}{dt} = -\frac{3}{8} \times f \times \frac{v \times v_x}{r} \times \frac{\rho}{\rho_w} \tag{1}$$

$$\frac{dv_y}{dt} = g \times \left(\frac{\rho}{\rho_w} - 1\right) - \frac{3}{8} \times f \cdot \frac{v \times v_y}{r} \times \frac{\rho}{\rho_w} \tag{2}$$

where v_x, v_y are the velocities in the x and y directions, respectively; v the velocity found from the two preceding components; f the friction factor depends of the Reynolds number [42]; ρ air density in ambient conditions; ρ_w water density; and r droplet radius. Droplet sizes should be smaller than 2 mm and higher than 20 microns to guarantee the non-evaporation of the water to be cooled in distances of less than 3 m. Above this size, according to Bird et al. [41], the formulation approach should be modified to take into account the mass transfer of the phenomenon. Moreover, the droplet radius is one of the model's essential parameters and it relates the above two equations to Equations (4) and (5) below.

It should be noted resistance force due to the friction effect as a drag force (Equation (3)). This drag force acts opposite to the direction of the oncoming flow velocity. The friction factor must be obtained by correlations. Qualitatively, it is clear that the smaller the radius, the shorter the time to reach the terminal velocity and the smaller it will be, as the relative importance of friction forces is greater. Earth speed is the speed of free fall that appears as a balance between the forces of gravity, buoyancy, and resistance. This end speed is a function of the radius of the drop.

$$F_f = -fxSxE_K \tag{3}$$

where S [m^2] is the frontal area to the movement, E_K [J/m^3] is the kinetic energy $\left(\frac{1}{2}\cdot\rho\cdot v^2\right)$ function of the velocity vi in the y-direction (v_y) or the x-direction (v_x); and f is the friction or drag coefficient. It can be seen how this force that is exerted has a friction component and a shape component by these two terms that are multiplied. Moreover, this factor f is inversely proportional to the speed for low Reynolds numbers and could be considered constant for high values of the same.

Droplet trajectory and global energy balance (Equation (4)) are coupled. However, the aim of this paper is cooling the water. Evaporation rate of the droplet is lower than 2% since droplet sizes are between 200–500 microns and flight height thereof is less than 3 m. So, global energy balance is computed with Equation (4) by analyzing the energy exchange induced by a variation in temperature. The energy exchanges involved in the system include convective transfer between the droplet and the air due to their temperature differential and evaporative transfer due to direct water–air contact. Energy exchanges due to surface tension and viscous dissipation, also present, can be disregarded as negligible compared in magnitude to the other two. The temperature variation of the drop is due to the transfer of heat by convection and to the evaporation itself. Energy exchanges have been neglected due to surface tension and viscous dissipation according to Hewitt et al. [43]. Equation (4) below expresses the global energy balance in the droplet:

$$\rho_w C_{Pw}.\frac{dT_w}{dt} = 3\frac{h}{r}(T_a - T_w) - \frac{3\rho x k_y}{r} x h_{lg} \frac{Y_{A0} - Y_{A\infty}}{1 - Y_{A0}} \tag{4}$$

where ρ_w is water density; C_{Pw} water specific heat; T_w droplet temperature at any given time; h heat transfer film coefficient; T_a air temperature; r droplet radius; ρ air density; k_y mass transfer coefficient; h_{lg} latent heat of vaporisation; Y_{A0} air mass fraction; and $Y_{A\infty}$ saturated air mass fraction.

The evaporation rate per square meter of drop surface (Equation (5)) must also be envisaged to factor in the effect of evaporation-induced radius shrinkage by Ficks's laws of diffusion:

$$\rho_w \frac{dr}{dt} = \rho k_y \frac{Y_{A0} - Y_{A\infty}}{1 - Y_{A0}} \tag{5}$$

where the variables are as described for Equation (4), and $\rho_w \frac{dr}{dt}$ is the mass transport per unit time and drop surface, that is connected with the reduction of its volume; ky is related with the Sherwood number [44] and it is possible to estimate using correlations. Some correlations make use of non-linear mathematical expressions and evaporation-convection can be linked. Cengel et al. [45] gave details of this heat and mass transfer.

As noted earlier, the solution to the detailed model described can be used to determine the essential parameters defining the droplet, namely radius and temperature, at any given time.

Droplet temperature can then be applied to define the efficiency of energy exchange at any given time. Energy exchange efficiency constitutes a very significant indicator of the performance of different cooling technologies in general and has been used as such [46], as well as for evaporative cooling [47,48]. Energy exchange efficiency in evaporative cooling is defined as the ratio between the actual variation in temperature in the droplet due to the cooling system and the maximum variation possible, i.e., to reach wet bulb temperature. It is calculated as shown in Equation (6):

$$\varepsilon = \frac{T_{wi} - T_{wt}}{T_{wi} - T_{wb}} \tag{6}$$

where T_{wi} is initial droplet temperature; T_{wt} droplet temperature at any given time; and T_{wb} the wet bulb temperature for given weather conditions.

3.2. Proposed Simplified Model

The detailed model for a single droplet described in Section 3.1 calls for information on the nozzle (droplet distribution depending on the initial radius for a given nozzle, mass fraction, etc.) which is difficult to glean from system manufacturers' catalogues. That raises a need for a simplified nozzle characterization model based on the theoretical fundamentals of the detailed model but in which the input data are readily found on manufacturers' datasheets. The aim is to enhance model applicability to the design and assessment of such solutions.

The simplified characterization model for evaporative mist cooling is based on energy exchange efficiency (Equation (5)), a widely used indicator of evaporative cooling system performance, as mentioned earlier.

An ε-NTU relationship equivalent to that used in evaporative cooling towers can be found for sprayers, where the process taking place can be likened to developments in such towers. In the NTU method (number of transfer units method) [44], the effectiveness is the ratio of the actual heat transfer rate to the maximum possible heat transfer rate and the NTU is related with the value of the heat transfer capacity of the exchanger. If NTU is high, the more closely the exchanger tends to its thermodynamic limit value. This method is commonly used for the characterization of evaporative cooling equipment [49–51]. The functional relationship associated with an exchanger is represented in efficiency calculations as term *A*, which depends on system operating variables. Efficiency can be calculated from Equation (7):

$$\varepsilon = 1 - e^{-NTU} = 1 - e^{-A} \tag{7}$$

where coefficient *A* is found from the system operating variables with a significant impact on cooling efficiency, measurable or furnished by manufacturers. On those grounds, the following parameters were applied to find parameter *A*:

- Factors depending on actual experimental conditions: outdoor temperature, absolute humidity, and initial droplet temperature.
- Factors with a role in evaporative cooling system operation: droplet launch height, working pressure, and droplet diameter.

In short, the simplified model proposed is linked to the treatment of the phenomenon as a heat dissipation system. So, determining the mathematical dependence of this parameter with the operating parameters of the system, Equations (1) to (4) have been implemented in Matlab [52]. These equations have been solved in a coupled way for thousands of combinations of boundary conditions. In this way, the mathematical formulation of parameter A that appears in Equation (7) is proposed. This formulation will be calibrated using experimental data, so it can be assumed that it is an instrumental step in the proposed methodology. As noted earlier, the simplified characterization model is designed for nozzles, not single droplets. Nozzles launch droplets of different sizes, creating a mist with water

particles of varying radii. Most nozzles spray droplets with a wide range of diameters, normally summarized via statistical analysis of the results of trials conducted with sophisticated measuring instruments, including laser analyzers and imaging systems. Further to that information, the droplets are classified on the grounds of a statistical distribution based on spraying pressure (see the paper by Thomas et al. [53]).

The diameter that qualifies nozzles for given rated working conditions is VMD or mean volumetric diameter, defined as the volume-median droplet diameter (the diameter for which half the total water content is contained in droplets larger and a half in droplets smaller than the median volume). Defined in standards and specific references such as [54,55], that widely used parameter is deemed to be the characteristic jet diameter. After entering the parameters into the simplified model, the effect of each of the aforementioned variables on evaporative cooling efficiency was analyzed. Applying the model to nozzles for which data were furnished in the literature [55], the variables could be localized in the numerator or denominator of the fraction (see Equation (5)) that make up the term A (see Equation (6)). The effect of each is illustrated in Figure 5 (see Equations (1)–(5) for more details about the definition of efficiency).
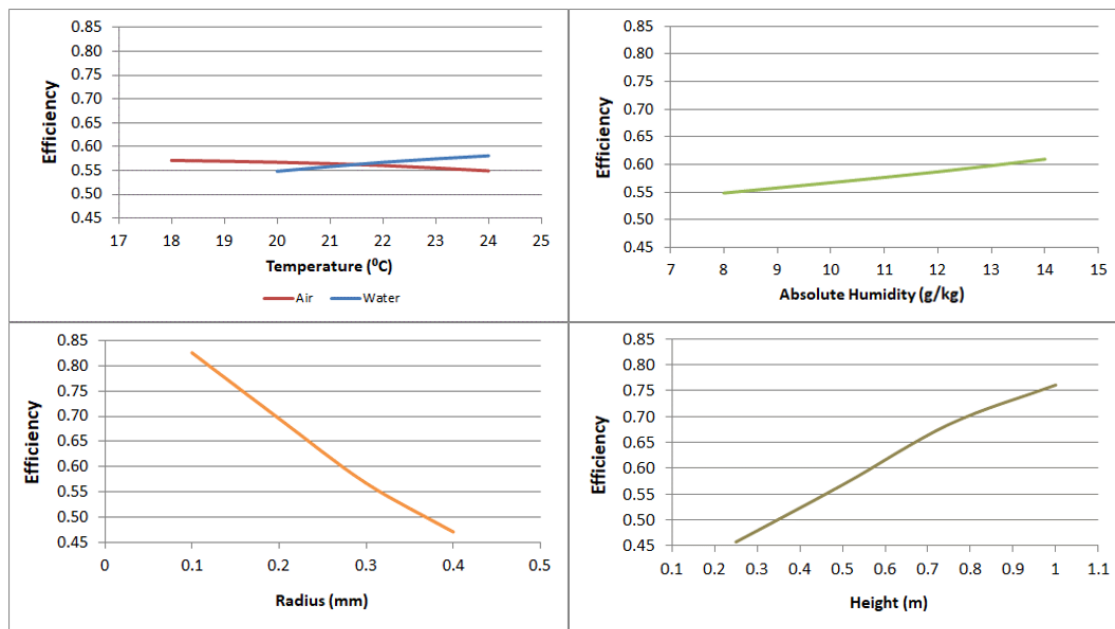

Figure 5. Effect of model variables on efficiency (see Equation (5)).

The findings graphed (these efficiencies have been estimated using the definition of Equation (5) in Figure 5 can be applied to develop the model proposed in Equation (6). The final proposal for the simplified model for characterizing nozzle efficiency from its operating parameters is set out in Equation (8):

$$\varepsilon = 1 - e^{\left(-\frac{Y_{ai} T_{wi} \dot{m}_w \sqrt{H\cdot}}{T_a x r_i} FT\right)} \tag{8}$$

where the terms of that equation, drawn from sprayer operation, are as follows: Y_{ai} is absolute humidity; T_{wi} initial water temperature; H nozzle height; $\dot{m}_w$ sprayer-propelled water flow; T_a outdoor temperature; and r_i representative droplet radius. This simplified model was calibrated using the results of the detailed single droplet model (Equations (1)–(4)) with the theoretical fitting factor FT, which is specific to nozzle and sprayer type and refers to the reduction of the detailed to the simplified model proposed. Its value must be stable and liable to being tabulated as shown in the results section.

The simplified nozzle characterization model developed (Equation (7)) is readily applicable using manufacturer data sheets and specific operating conditions.

3.3. Model Calibration

The model proposed to characterize elements of evaporative cooling is based on a theoretical formulation that yields an empirical equation and its subsequent correction to neutralize the hypotheses assumed to formulate the model. The hypotheses primarily inducing model deviation from reality are that a nozzle can be equated to a water droplet with a representative radius defined by the largest volumetric fraction and that inter-droplet interaction can be ignored.

The experiments conducted with the two case study nozzles, HARDI ISO F-110-04 and HARDI ISO F-110-06, served as grounds for validating the proposed model and correcting for the hypotheses assumed in its formulation.

Model calibration was based on the experiments described in Section 2.4. The model had to be corrected as far as possible before entering the actual effect of the variables concerned to be able to characterize the performance of the elements studied. The starting point for all the sprayers was Equation (7), where the theoretical fitting factor, *FT*, varied depending on the sprayer type and model. The final step in the procedure proposed is to extrapolate formulation of Equation (7) to estimate efficiency of evaporative dissipation system using Equation (9). The result was the simplified model corrected with experimental factor *FC*, which in turn depends on the operating conditions:

$$\varepsilon_D == 1 - e^{\left(-\frac{Y_{ai}T_{wi}\dot{m}_{tw}\sqrt{H\cdot}}{T_a \times r_i}FTxFC\right)} \tag{9}$$

where ε_D is the efficiency of the evaporative dissipation system and it is calculated according to Equation (9). Correction factor *FC* has the same meaning as fitting factor *FT* discussed in connection with Equation (7) but must be obtained experimentally. Two possibilities were tested in this study: obtaining a theoretical fitting factor *FT* from the detailed model and subsequently calibrating the Equation (7) model with the experimental correction factor, and assuming the theoretical fitting factor to be equal to 1 and calibrating the experimental data model with correction factor *FC*. Both options guarantee suitable results. The first delivers a more robust model for application outside the range of the experimental data used for calibration and validation. With option 2, in turn, there is no need to implement the detailed model, although the quality of the estimates depends on the amount of experimental data used for correction (weather variability and operating conditions).

FT is used to reduce the detailed model (Equations (1)–(5)) to de simplified model (Equation (8)). However, estimation of Equation (8) has to be calibrated using experimental data. This calibration is done using the FC parameter in Equation (9). So, estimation of efficiency should be done under real conditions. Equation (8) is defined using simulation results, but the estimation of Equation (9) is going to be compared with real data. Real conditions involve variable and difficult to measure excitations and heat fluxes. So, it proposes to use the reference pond to measure the net effect of heat dissipation by experiment using this dissipation technique. For that, the efficiency of dissipation system is defined using Equation (9):

$$\varepsilon_D = \frac{\Delta T_W}{T_{iWP} - \overline{T_{wb}}} \tag{10}$$

where T_{iWP} is the initial temperature (°C) of water in reference and evaporative ponds; $\overline{T_{wb}}$ is the average of wet-bulb temperature (°C) during experimental sampling (in this case is two hours), and ΔT_W is the difference temperature between the average water temperature between reference and evaporative ponds at the end of experimental sampling. This difference ΔT_W between the temperature of two ponds is due to the operation of the dissipation system. Since both cells are assumed to be subjected under the same convective, radiant, and conduction climatic conditions. As explained in Section 2, this is the way proposed in the methodology to explicitly take into account the rest of unmeasured climatic excitations: build a reference prototype with which to compare the system under study.

The results section shows how the deviation observed in the theoretical simplified model (Equation (8)) could be corrected with the procedure proposed as per Equation (9). That approach guaranteed deviation of under 5% in all cases, as attested to by the results discussed in the following section.

4. Results and Discussion

The findings for the experiments described in Section 3.3 are set out below.
The tests run were classified by the aim pursued:

- Experiment 1: assessment of thermal loss in the ponds.
- Experiment 2: analysis of cooling power and the development, calibration, and validation of the simplified model proposed.
- Experiment 3: analysis of the sensitivity of the parameters for the simplified model proposed.

4.1. Experiment 1

As noted in an earlier section, experiment 1 was designed to assess thermal loss in the two ponds, only one of which (evaporative pond) was fitted with sprayers. The aim was to ensure that thermal loss was identical in it and the reference pond to be able to compare their actual respective cooling power. Figures 6 and 7 show experimental results of the comparison between evaporative pond and reference pond under the same weather conditions.

To conduct the experimental assessment, the starting temperature had to be the same in the two ponds. The water in the two was consequently intermixed at the beginning of the experiment and subsequently heated to 27 °C, after which the temperature was allowed to fluctuate freely, i.e., with the sprayers idle.
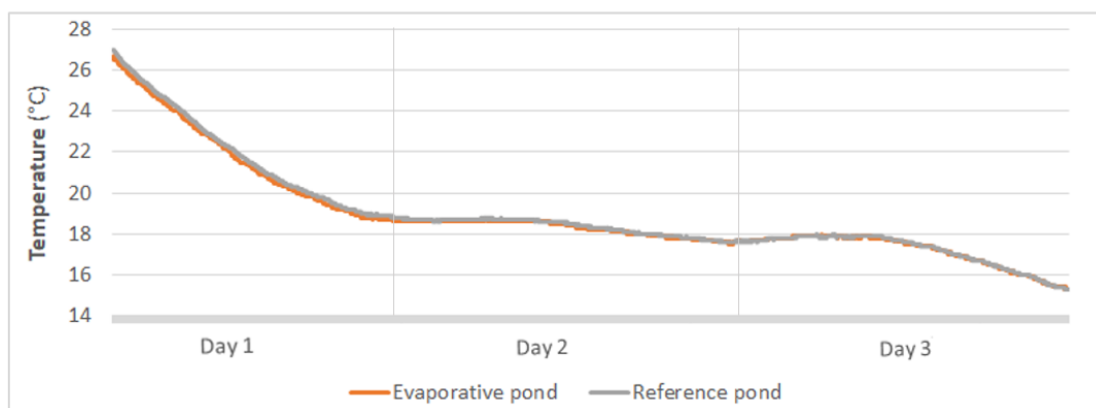

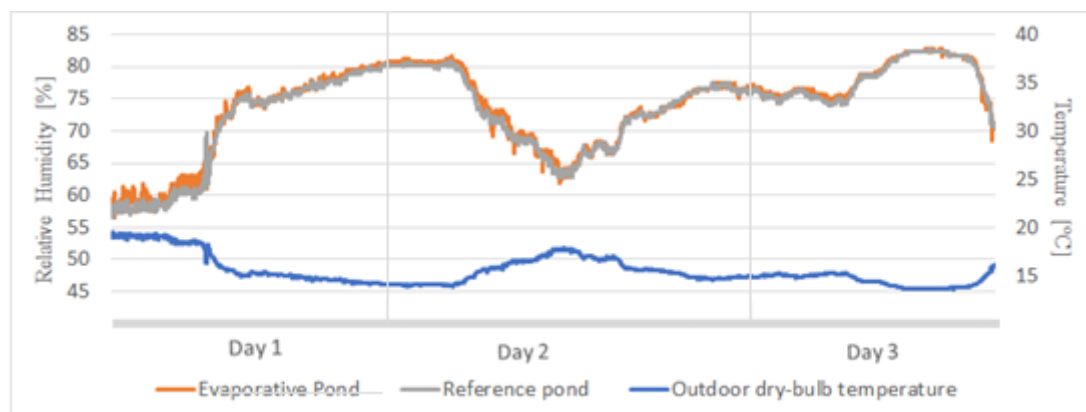**Figure 6.** Water temperature fluctuation in the ponds (experiment 1).

Figure 7. Relative humidity and dry-bulb temperature fluctuation in the ponds (experiment 1).

Relative humidity in the vicinity of the two ponds was also similar in both, as Figure 7 shows.

As the thermal fluctuation of the water in the two ponds in the first three days of the first week (see Table 1) shows (Figure 1), the temperature was consistently the same in both. The graph illustrates the utility of the reference pond, for it denotes the temperature of the evaporative pond water in the absence of the cooling system. It, therefore, constitutes a baseline, an imperative found in all comparative studies in the literature.

Since the two ponds exhibited identical thermal and humidity responses to the same conditions, any differences in cooling power could be validly attributed to the use of sprayers in one and their absence in the other.

4.2. Experiment 2

Experiment 2 yielded two sets of findings: on the one hand the empirical results and on the other the validation and calibration of the proposed model. They are discussed separately below.

4.2.1. Experiment 2 Results

The results of comparing evaporative mist cooling power with each of the two nozzles to unaided evaporation-governed cooling in a pond not fitted with sprayers are discussed below.

The temperature fluctuations from 22.00 to 06:00 on day 3 of experiment week 2 (see Table 1) in the reference pond and in the evaporative pond with the HARDI ISO F-110-04 nozzles on are compared in Figure 8, which shows that by the end of the operating period, the temperature in the latter was 6 °C lower than in the former, verifying a rise in cooling power attributable to the use of sprayers.
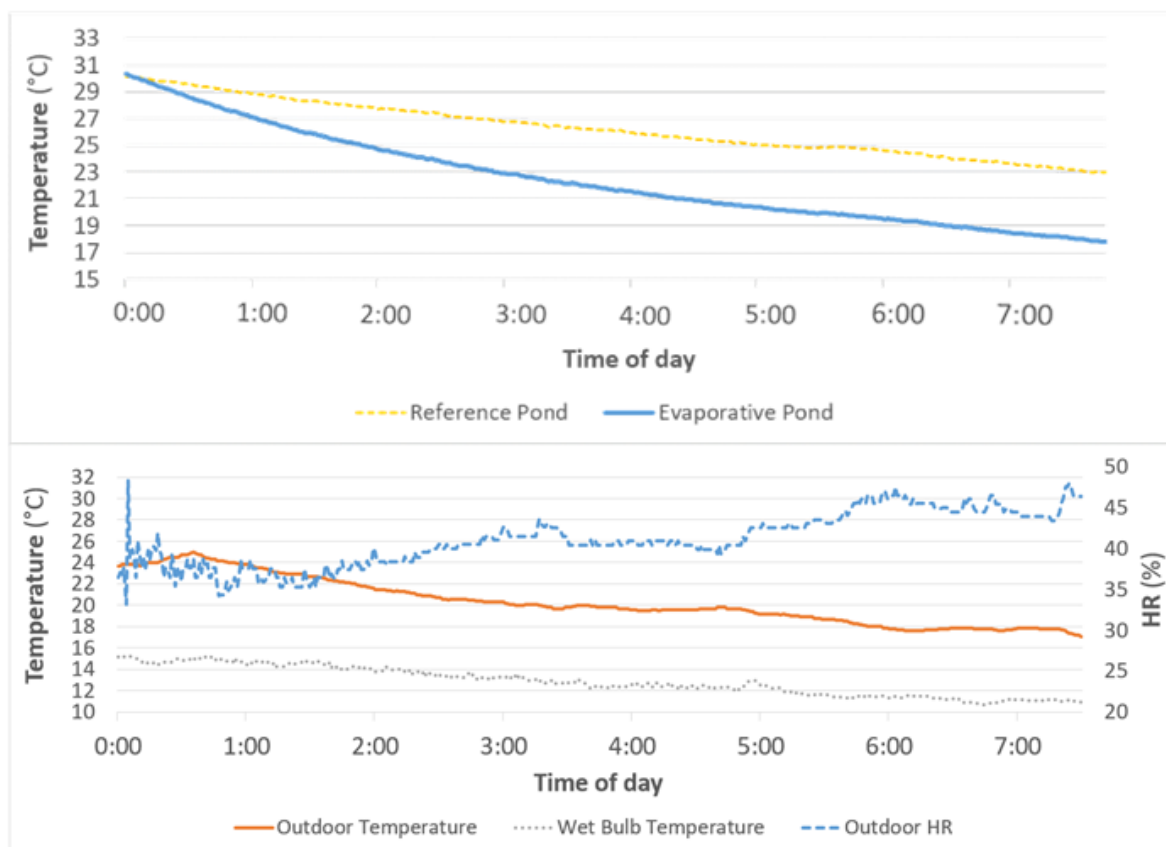

Figure 8. Water temperature fluctuations in the reference pond and the evaporative pond with HARDI ISO F-110-04 nozzles (**up**) and environmental conditions: dry-bulb temperature, wet-bulb temperature, and humidity ratio HR (**down**).

Figure 9 compares the performance of the reference pond and the evaporative pond fitted with HARDI ISO F-110-06 nozzles in week 3, in the same 8 h period as in Figure 8. The evaporative pond temperature with the HARDI ISO F-110-06 nozzle was just 2.5 °C lower than in the reference pond, a notably narrower difference than with the other nozzle type.
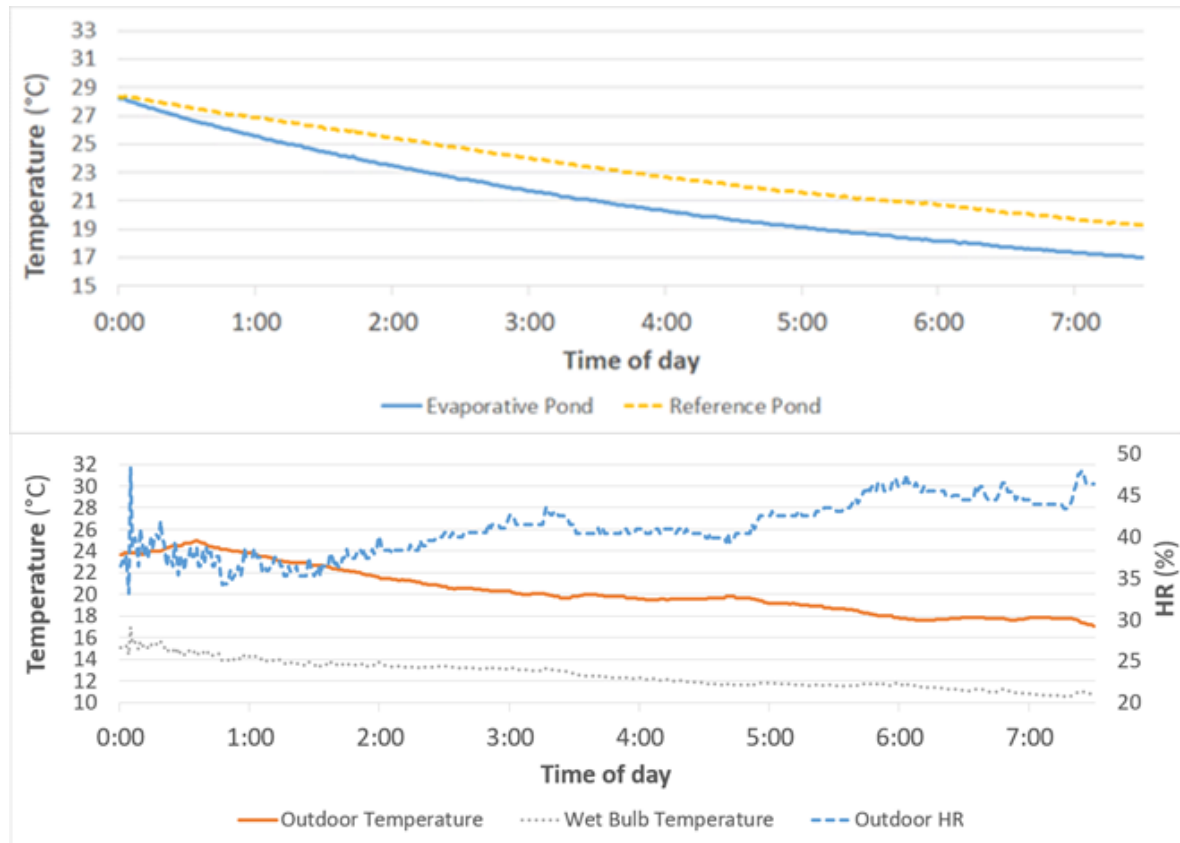

Figure 9. Water temperature fluctuations in the reference pond and in the evaporative pond with HARDI ISO F-110-06 nozzles (**up**) and environmental conditions: dry-bulb temperature, wet-bulb temperature, and humidity ratio HR (**down**).

Figure 10 shows the mean cooling power of the two types of the nozzle across the two weeks of experiment 2. The energy dissipated was calculated with Equation (9), in which pond cooling power was found as the difference between the decline in temperature in the evaporative pond less the decline in the reference pond; thereby, limiting the result to actual cooling power and excluding other possible factors such as the water film coefficient:

$$Dissipated\ energy = m_{water-pond} \cdot CP_w \cdot \left(\Delta T_{evaporaative} - \Delta T_{reference} \right) \quad (11)$$

where $m_{water-pond}$ is the mass of the water in one of the ponds; CP_w the calorific value of the water under the conditions in place; ∇T_{sprays} the daily difference in temperature in the evaporative pond; and $\nabla T_{reference}$ the daily difference in temperature in the reference pond. Equation (9) can also be applied hourly to find dissipation efficiency on an hourly basis.

As Figure 10 shows, mean energy dissipation was higher in the week (week 2, Table 1) when the HARDI ISO F-110-04 nozzle was used, as would be expected, for as the droplet diameter was smaller and contact area consequently larger, heat transfer was more effective.
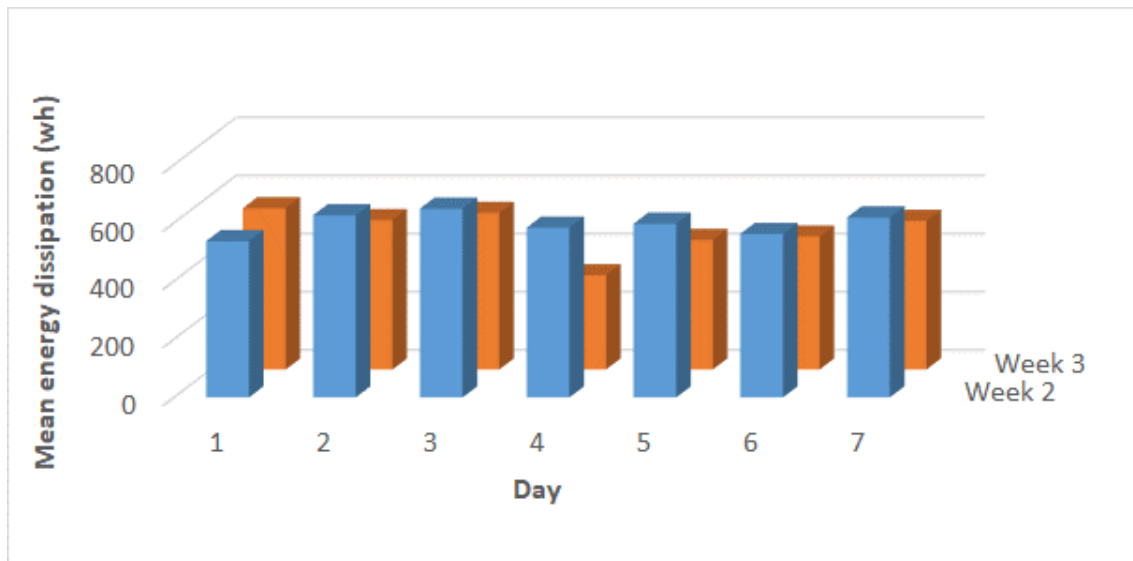
Figure 10. Mean energy dissipation, experiment 2.

4.2.2. Validation and Calibration of the Simplified Characterization Model Proposed

The validation and calibration findings for the simplified characterization model proposed to assess and design evaporative mist cooling systems based on experiment 2 empirical assessment are discussed below.

Generally speaking, for both nozzles the correction factor was found from the data for five days of the week and the model validated with the data for the remaining two days.

The first step in the procedure was to calculate evaporative cooling efficiency by entering the experiment 2 findings into Equation (5) (Section 3), and subsequently determine the efficiency with the characterization model proposed, as formulated in Equation (7) (Section 3). Applying the procedure first to nozzle HARDI ISO F-110-04 yielded an FT theoretical fitting factor of 0.034.

As Figure 11 shows, the empirical findings differed from the simplified characterization model results. To narrow that difference, the model was corrected with factor FC, described in Section 3.3. The calibrated model, as expressed in Equation (8) in the aforementioned item, yielded a correction factor for nozzle HARDI ISO F-110-04 of 0.941. So, FC is obtained by the minimization of the differences between the estimation of efficiency using Equation (8) and the real value measured (Equation (9)). FC is the optimum value for which this difference is the minimum.

Figure 12, in turn, shows the empirical and model results for the HARDI ISO F-110-06 cooling efficiency. Here correction factor FC (Equation (8)) was 0.975 and the theoretical fitting factor FT (Equation (7)) 0.034.

Model fitting factor FT and correction factor FC were found using two hourly values in the first five days of the week the experiment was conducted.

The values of the correction factors proposed were consistently close to 1: 0.941 for HARDI ISO F-110-04 and 0.975 for HARDI ISO F-110-06. The fitting factor FT, in turn, was stable at 0.034 in both cases, varying only at the fourth decimal place.
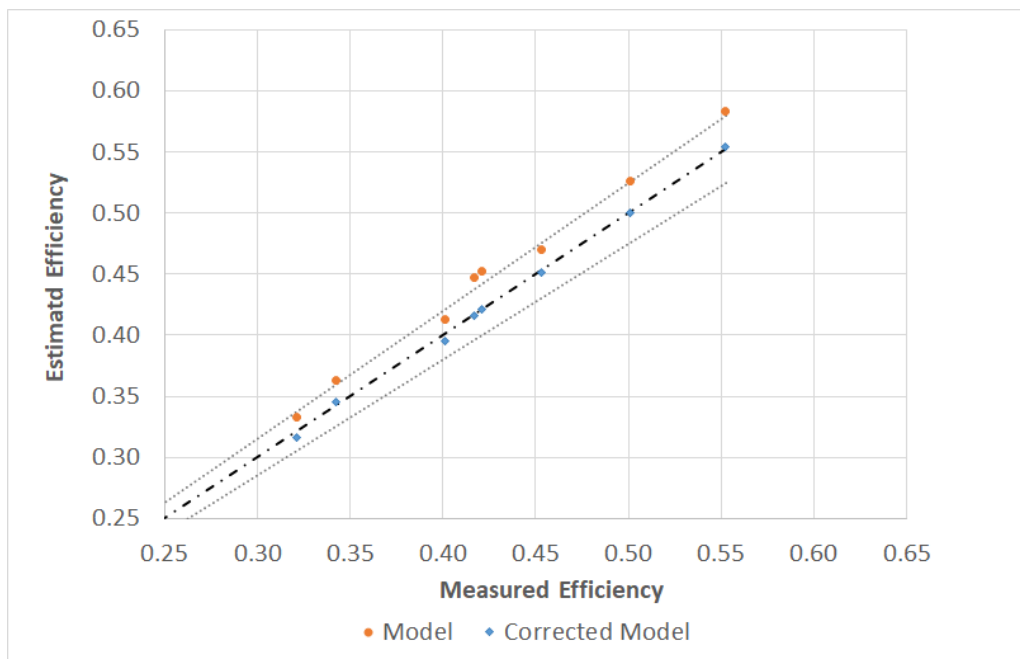
Figure 11. Validation and calibration of the model for HARDI ISO F-110-04 nozzles.
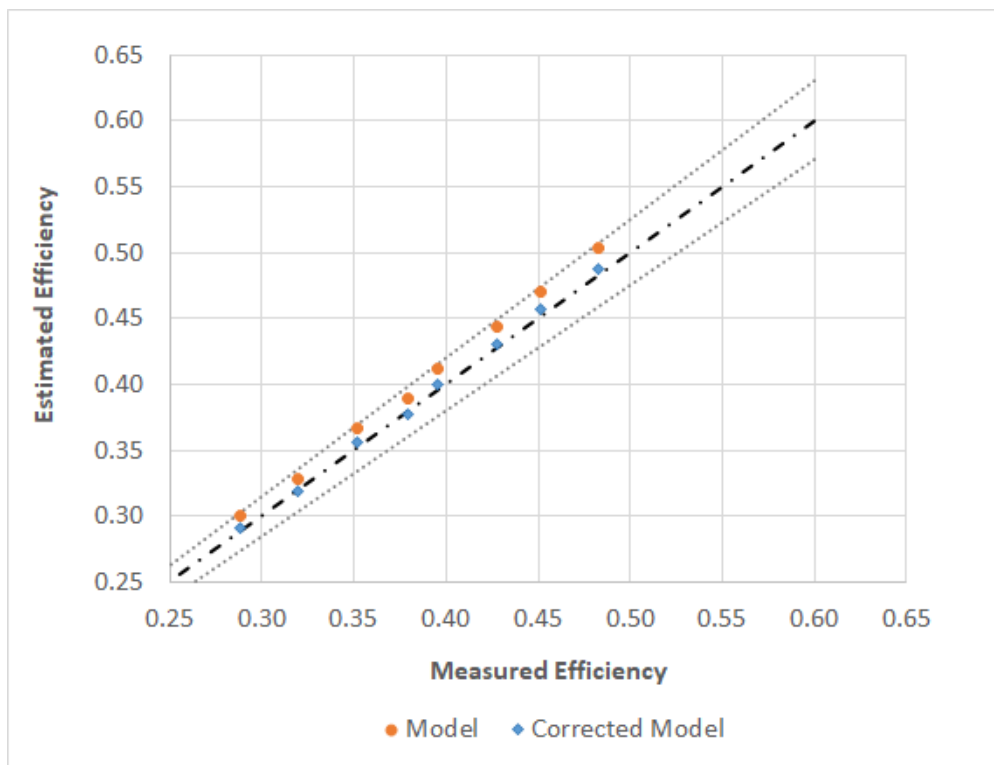

Figure 12. Validation and calibration of the model for HARDI ISO F-110-06 nozzles.

4.3. Experiment 3

An analysis was run on the validated and calibrated simplified characterization model developed on the grounds of empirical findings to determine model sensitivity to the input variables. Experiment 3 was consequently designed to analyze the effect of the model variables with an impact on system

performance. More specifically, nozzle height and pressure were the two parameters analysed based on the findings for weeks 4 and 5. The figures below give the daily mean values.

Figure 13 graphs the variation in mean cooling efficiency with nozzle height. Changes in height entailed differences in droplet travel distance and with it residence time or the time the droplet was suspended in air. Consequently, the higher the nozzle, the longer the travel distance and residence time, which raised efficiency. The maximum height was set at 0.6 m to reduce the number of droplets travelling horizontally due to wind action.
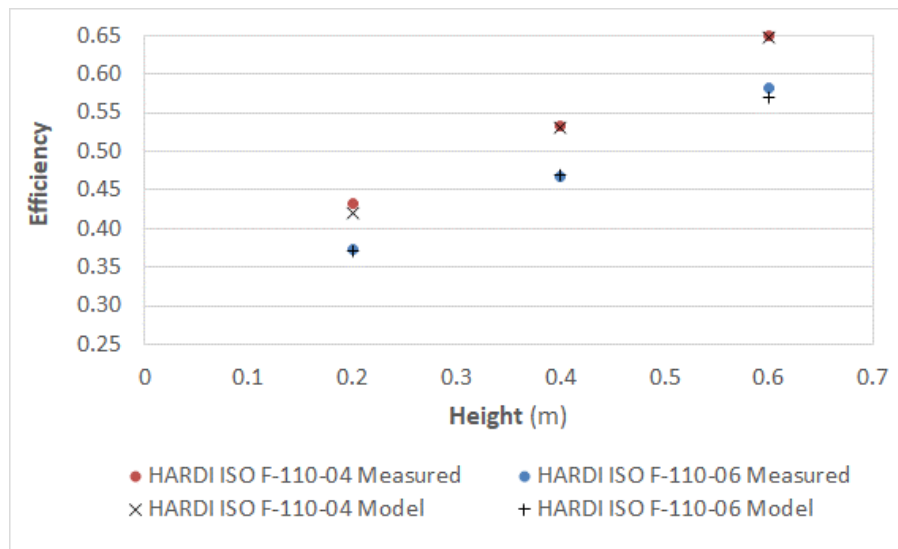

Figure 13. Variation in mean cooling efficiency vs. nozzle height.

The variation in mean cooling efficiency with working pressure is shown in Figure 14, using manufacturer-specified values [39]. Pressure had a direct effect on nozzle flow and droplet scatter, as Figure 14 shows, with efficiency rising with pressure. More specifically, pressure affected the rate at which the water cooled.
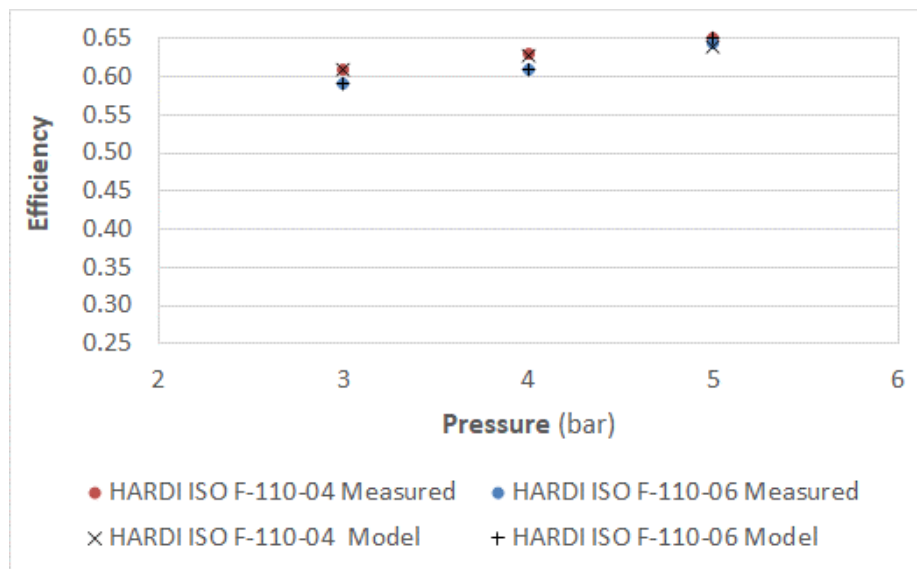

Figure 14. Variation in mean cooling efficiency vs. working pressure.

Table 2 summarizes mean overnight cooling efficiency as calculated from Equation (9) for each day of the experiment, excluding week 1, based on the variables affecting the proposed model and the simplified, experimentally validated model for the two nozzles.

The data show that efficiency was greatest where sprayer height and working pressure were highest.

Table 2. Mean daily efficiency.

	Day 1	Day 2	Day 3	Day 4	Day 5	Day 6	Day 7
Week 1	EXPERIMENT 1						
Week 2	Experiment 2	Experiment 2	Experiment 2	Experiment 2	Experiment 2	Experiment 2	Experiment 2
	0.51	0.57	0.59	0.53	0.54	0.52	0.56
Week 3	Experiment 2	Experiment 2	Experiment 2	Experiment 2	Experiment 2	Experiment 2	Experiment 2
	0.52	0.50	0.51	0.38	0.47	0.49	0.50
Week 4	Experiment 3	Experiment 3	Experiment 3	Experiment 3	Experiment 3	Experiment 3	Experiment 3
	0.43	0.53	0.65	0.64	0.68	0.70	0.37
Week 5	Experiment 3	Experiment 3	Experiment 3	Experiment 3	Experiment 3		
	0.47	0.58	0.61	0.66	0.68		

The percentage of water evaporating overnight graphed in Figure 15 for all seven days in weeks 2 through 5 shows that water loss from the ponds was no greater than 6% on any of the days tested. That value is equivalent to a mean loss of 2 L/h during the month, less than reported in other studies on evaporative cooling, according to Kabeel et al. [56]. The findings not only validated the efficiency of this passive natural cooling technique but also ruled out the hypothesis that such systems entail high water consumption.
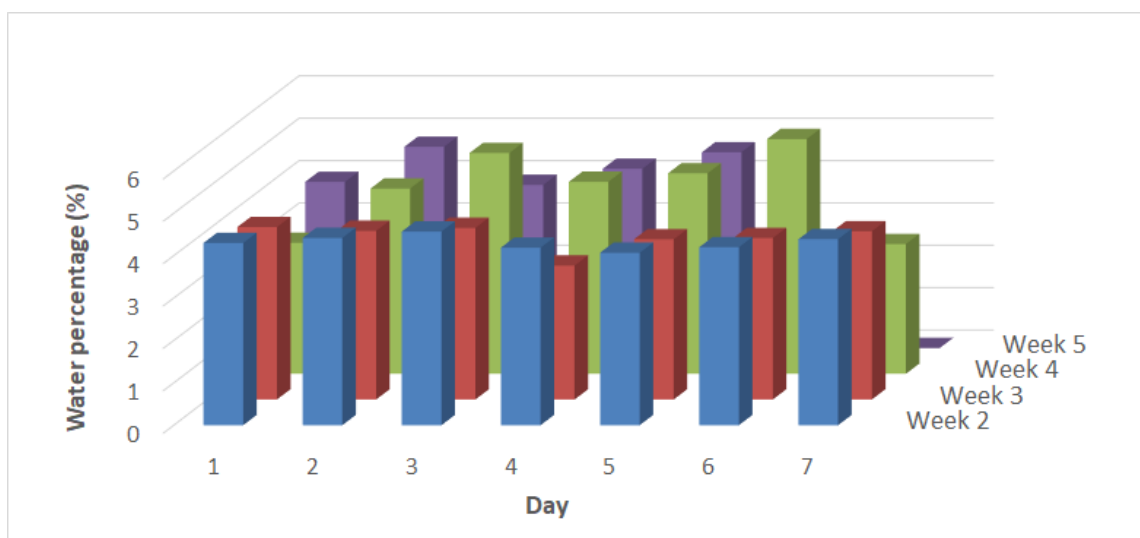

Figure 15. Daily evaporation (%).

Water consumption is a prominent variable in evaporative cooling technique analysis, as discussed by other authors seeking to lower that parameter [57,58]. The specific consumption (consumption/energy dissipated) found here lay within the range reported in the aforementioned papers.

5. Conclusions

Water is a natural heat sink with high cooling power. This study characterized and thermally assessed the water cooling technique used in an evaporative system in which water was regarded as a bioclimatic vehicle to air condition spaces. To that end, efficiency was adopted as an indicator and a simplified model developed with experimental data was proposed to determine its value. Experimental validation of the model yielded errors of under 5%.

The present findings confirm the potential to lower water temperature evaporatively. Coldwater can be used to air condition in different applications. The most prominent conclusions drawn from this study are listed below:

- The simplified model proposed was calibrated and validated on the grounds of extensive experimentation. The model uses operating variables as input, facilitating decision-making.
- The methodology described is applicable to other types of sprayers provided the technical specifications, which can be found on all manufacturers' datasheets, are known.
- Mean cooling power is on the order of 500 Wh, with overnight energy dissipation ranging from 2.6 kWh to 6.0 kWh (see Figure 10), depending on the experiment, with an associated evaporation-governed decline in the range temperature of 2 °C to 6 °C. In the experimental setup designed to measure system impact directly, consisting of two identical ponds exposed to the same environmental conditions, one could be used as a reference to determine the thermal impact of evaporative dissipation.
- No more than 6% of the ponded water evaporated under any of the conditions studied, whilst mean evaporation amounted to 4% (see Figure 15).

At around 60%, the experimental results for mean efficiency found for this natural evaporative mist cooling system are more reliable than the 80% to 90% generally cited in the literature. The simplified model developed from those experimental findings, in conjunction with the methodology, which is designed for analyzing new manufacturers and changing climates, can be applied in future studies to assess building energy efficiency.

Finally, dissipation systems based on evaporative techniques have high energy performance. It is common to find them coupled to chiller capacitors. However, its integration through pond is unusual. Installation costs for this technology are low, but operation and maintenance costs can be considerable. There is a consumption of water, which, even though it is not high, can reduce its applicability on in this situation with a scarcity of this resource. Maintenance is a critical point since it is necessary to control the quality of the water and avoid the appearance of microorganisms. It can cause unpleasant odors, loss of aesthetics and even diseases. Likewise, the possibilities of freezing these systems in cold regions must be taken into account in the design. Nozzles are inexpensive, but water hardness can be a problem after a long period of operation. Even with this, these techniques are one of the best solutions for the natural production of cold water.

Conflicts of Interest: The authors declare no conflict of interest.

Nomenclature

Variable	Description	Unit
vx	Droplet velocity in x direction	m/s
vx	Droplet velocity in y direction	m/s
f	Darcy friction factor	-
v	Droplet velocity	m/s
ρ	Air density	kg/m^3
ρ_w	Water density	kg/m^3
r	Droplet radius	m
g	Gravitational acceleration	m/s^2
Ff	Friction or drag force	N
S	Frontal area of drop	m^2
Ki	Kinetics energy of drop	J
$CP_{w\cdot}$	Specific heat of water	kJ/kg·K
T_w	Droplet temperature	°C
h	Film coefficient	W/mK
T_a	Air temperature	°C
k_y	Global heat transfer coefficient	m/s
h_{lg}	Latent heat of vaporization	kJ/kg
Y_{A0}	Air mass fraction	kg/kg
$Y_{A\infty}$	Saturated air mass fraction	kg/kg
ε	Efficiency	-
mwt	Return water flow rate	kg/s
mwi	Initial water flow rate	kg/s
Twi	Initial water temperature	°C
Twt	Return water temperature	°C
Twb	Wet bulb temperature	°C
Yai	Absolute humidity	g/kg
H	Spray tower height	m
Fc	Model-empirical correction factor	-
T_{ip}	Initial evaporative pond temperature	°C
T_{op}	Final evaporative pond temperature	°C
T_{ipr}	Initial reference pond temperature	°C
T_{opr}	End reference pond temperature	°C
Qcool	Cooling power	W

References

1. Santamouris, M. Innovating to zero the building sector in Europe: Minimising the energy consumption, eradication of the energy poverty and mitigating the local climate change. *Sol. Energy* **2016**, *128*, 61–94. [CrossRef]
2. Santamouris, M. Cooling the buildings—Past, present and future. *Energy Build.* **2016**, *128*, 617–638. [CrossRef]
3. Asimakopoulos, D.A.; Santamouris, M.; Farrou, I.; Laskari, M.; Saliari, M.; Zanis, G.; Giannakidis, G.; Tigas, K.; Kapsomenakis, J.; Douvis, C.; et al. Modelling the energy demand projection of the building sector in Greece in the 21st century. *Energy Build.* **2012**, *49*, 488–498. [CrossRef]
4. Mohajerani, A.; Bakaric, J.; Jeffrey-Bailey, T. The urban heat island effect, its causes, and mitigation, with reference to the thermal properties of asphalt concrete. *J. Environ. Manag.* **2017**, *197*, 522–538. [CrossRef] [PubMed]
5. Jato-Espino, D. Spatiotemporal statistical analysis of the Urban Heat Island effect in a Mediterranean region. *Sustain. Cities Soc.* **2019**, *46*, 101427. [CrossRef]
6. Bhamare, D.K.; Rathod, M.K.; Banerjee, J. Passive cooling techniques for building and their applicability in different climatic zones—The state of art. *Energy Build.* **2019**, *198*, 467–490. [CrossRef]

7.　Givoni, B. Indoor temperature reduction by passive cooling systems. *Sol. Energy* **2011**, *85*, 1692–1726. [CrossRef]

8.　Santamouris, M.; Pavlou, K.; Synnefa, A.; Niachou, K.; Kolokotsa, D. Recent progress on passive cooling techniques: Advanced technological developments to improve survivability levels in low-income households. *Energy Build.* **2007**, *39*, 859–866. [CrossRef]

9.　Chiesa, G.; Grosso, M.; Pearlmutter, D.; Ray, S. Advances in adaptive comfort modelling and passive/hybrid cooling of buildings. *Energy Build.* **2017**, *148*, 211–217. [CrossRef]

10.　Yu, F.W.; Chan, K.T. Economic benefits of optimal control for water-cooled chiller systems serving hotels in a subtropical climate. *Energy Build.* **2010**, *42*, 203–209. [CrossRef]

11.　Cheung, H.; Wang, S. Reliability and availability assessment and enhancement of water-cooled multi-chiller cooling systems for data centers. *Reliab. Eng. Syst. Saf.* **2019**, *191*, 106573. [CrossRef]

12.　Huang, P.; Huang, G.; Augenbroe, G.; Li, S. Optimal configuration of multiple-chiller plants under cooling load uncertainty for different climate effects and building types. *Energy Build.* **2018**, *158*, 684–697. [CrossRef]

13.　Zhou, X.; Liu, Y.; Luo, M.; Zhang, L.; Zhang, Q.; Zhang, X. Thermal comfort under radiant asymmetries of floor cooling system in 2 h and 8 h exposure durations. *Energy Build.* **2019**, *188*, 98–110. [CrossRef]

14.　Tang, H.; Zhang, T.; Liu, X.; Jiang, Y. Novel method for the design of radiant floor cooling systems through homogenizing spatial solar radiation distribution. *Sol. Energy* **2018**, *170*, 885–895. [CrossRef]

15.　Zhao, K.; Liu, X.H.; Jiang, Y. Application of radiant floor cooling in large space buildings—A review. *Renew. Sustain. Energy Rev.* **2016**, *55*, 1083–1096. [CrossRef]

16.　Lehmann, B.; Dorer, V.; Gwerder, M.; Renggli, F.; Tödtli, J. Thermally activated building systems (TABS): Energy efficiency as a function of control strategy, hydronic circuit topology and (cold) generation system. *Appl. Energy* **2011**, *88*, 180–191. [CrossRef]

17.　Park, S.H.; Chung, W.J.; Yeo, M.S.; Kim, K.W. Evaluation of the thermal performance of a Thermally Activated Building System (TABS) according to the thermal load in a residential building. *Energy Build.* **2014**, *73*, 69–82. [CrossRef]

18.　Gao, J.; Li, A.; Xu, X.; Gang, W.; Yan, T. Ground heat exchangers: Applications, technology integration and potentials for zero energy buildings. *Renew. Energy* **2018**, *128*, 337–349. [CrossRef]

19.　Soni, S.K.; Pandey, M.; Bartaria, V.N. Ground coupled heat exchangers: A review and applications. *Renew. Sustain. Energy Rev.* **2015**, *47*, 83–92. [CrossRef]

20.　Wu, W.; Li, X.; You, T.; Wang, B.; Shi, W. Combining ground source absorption heat pump with ground source electrical heat pump for thermal balance, higher efficiency and better economy in cold regions. *Renew. Energy* **2015**, *84*, 74–88. [CrossRef]

21.　Hanif, M.; Mahlia, T.M.I.; Zare, A.; Saksahdan, T.J.; Metselaar, H.S.C. Potential energy savings by radiative cooling system for a building in tropical climate. *Renew. Sustain. Energy Rev.* **2014**, *32*, 642–650. [CrossRef]

22.　Meir, M.G.; Rekstad, J.B.; LØvvik, O.M. A study of a polymer-based radiative cooling system. *Sol. Energy* **2002**, *73*, 403–417. [CrossRef]

23.　Khedari, J.; Waewsak, J.; Thepa, S.; Hirunlabh, J. Field investigation of night radiation cooling under tropical climate. *Renew. Energy* **2000**, *20*, 183–193. [CrossRef]

24.　Hollick, J. Nocturnal radiation cooling tests. *Energy Procedia* **2012**, *30*, 930–936. [CrossRef]

25.　Bagiorgas, H.S.; Mihalakakou, G. Experimental and theoretical investigation of a nocturnal radiator for space cooling. *Renew. Energy* **2008**, *33*, 1220–1227. [CrossRef]

26.　Tewari, P.; Mathur, S.; Mathur, J. Thermal performance prediction of office buildings using direct evaporative cooling systems in the composite climate of India. *Build. Environ.* **2019**, *157*, 64–78. [CrossRef]

27.　Chiesa, G.; Grosso, M. Direct evaporative passive cooling of building. A comparison amid simplified simulation models based on experimental data. *Build. Environ.* **2015**, *94*, 263–272. [CrossRef]

28.　He, J.; Hoyano, A. Experimental study of practical applications of a passive evaporative cooling wall with high water soaking-up ability. *Build. Environ.* **2011**, *46*, 98–108. [CrossRef]

29.　Berardi, U.; La Roche, P.; Almodovar, J.M. Water-to-air-heat exchanger and indirect evaporative cooling in buildings with green roofs. *Energy Build.* **2017**, *151*, 406–417. [CrossRef]

30.　Manteghi, G.; bin Limit, H.; Remaz, D. Water Bodies an Urban Microclimate: A Review. *Mod. Appl. Sci.* **2015**, *9*, 1. [CrossRef]

31.　Domínguez, S.A.; Sánchez, F.J. *The Effect of Evaporative Techniques on Reducing Urban Heat. Urban Climate Mitigation Techniques*; Routledge: London, UK, 2016. [CrossRef]

32. Kleerekoper, L.; van Esch, M.; Salcedo, T.B. How to make a city climate-proof, addressing the urban heat island effect. *Resour. Conserv. Recycl.* **2012**, *64*, 30–38. [CrossRef]

33. Yamada, H.; Yoon, G.; Okumiya, M.; Okuyama, H. Study of cooling system with water mist sprayers: Fundamental examination of particle size distribution and cooling effects. *Build. Simul.* **2008**, *1*, 214–222. [CrossRef]

34. Yoon, G. Study on a cooling system using water mist sprayers; system control considering outdoor environment. In Proceedings of the Korea-Japan Joint Symposium on Human-Environment Systems, Cheju, Korea, 30 November 2008.

35. Nunes, J.; Zoilo, I.; Jacinto, N.; Nunes, A.; Campos, T.; Pacheco, M.; Fonseca, D. *Misting-Cooling Systems for Microclimatic Control in Public Space*; PROAP Landscape Architects: Lisbon, Portugal, 2016.

36. Bishoyi, D.; Sudhakar, K. Experimental performance of a direct evaporative cooler in composite climate of India. *Energy Build.* **2017**, *153*, 190–200. [CrossRef]

37. Camargo, J.R.; Ebinuma, C.D.; Silveira, J.L. Experimental performance of a direct evaporative cooler operating during summer in a Brazilian city. *Int. J. Refrig.* **2005**, *28*, 1124–1132. [CrossRef]

38. Elgendy, E.; Mostafa, A.; Fatouh, M. Performance enhancement of a desiccant evaporative cooling system using direct/indirect evaporative cooler. *Int. J. Refrig.* **2015**, *51*, 77–87. [CrossRef]

39. Manufacturer Catalogue. Agroparts. 2011. Available online: www.hardi-international.com (accessed on 6 August 2020).

40. Santamouris, M.; Kolokotsa, D. (Eds.) *Urban Climate Mitigation Techniques*; Routledge: London, UK, 2016. [CrossRef]

41. Bird, R.B.; Stewart, W.E.; Lightfoot, E.N. *Transport Phenomena*; John Wiley & Sons: New York, NY, USA, 2006; ISBN 978-0-470-11539-8.

42. Torobin, L.B.; Gauvin, W.H. Fundamental aspects of solids-gas flow: Part I: Introductory concepts and idealised sphere motion in viscous regime. *Can. J. Chem. Eng.* **1959**, *37*. [CrossRef]

43. Hewitt, G.F.; Delhaye, J.M.; Zuber, N. *Multiphase Science and Technology*; Hemisphere Publishing: New York, NY, USA, 1986; Volume 3, ISBN 0-89116-561-4. [CrossRef]

44. Bergman, T.L.; Incropera, F.P. *Fundamentals of Heat and Mass Transfer*; Wiley: Hoboken, NJ, USA, 2011; ISBN 0470501979.

45. Cengel, Y.; Ghajar, A. *Heat and Mass Transfer*, 5th ed.; McGraw-Hill Higher Education: New York, NY, USA, 2015.

46. Guan, M.; Annaheim, S.; Li, J.; Camenzind, M.; Psikuta, A.; Rossi, R.M. Apparent evaporative cooling efficiency in clothing with continuous perspiration: A sweating manikin study. *Int. J. Therm. Sci.* **2019**, *137*, 446–455. [CrossRef]

47. Fouda, A.; Melikyan, Z. A simplified model for analysis of heat and mass transfer in a direct evaporative cooler. *Appl. Therm. Eng.* **2011**, *31*, 932–936. [CrossRef]

48. Baca, I.M.; Tur, S.M.; Gonzalez, J.N.; Román, C.A. Evaporative cooling efficiency according to climate conditions. *Procedia Eng.* **2011**, *21*, 283–290. [CrossRef]

49. Mansour, M.K. Practical effectiveness-NTU model for cooling and dehumidifying coil with non-unit Lewis Factor. *Appl. Therm. Eng.* **2016**, *100*, 1111–1118. [CrossRef]

50. Gao, W.; Worek, W.; Konduru, V.; Adensin, K. Numerical study on performance of a desiccant cooling system with indirect evaporative cooler. *Energy Build.* **2015**, *86*, 16–24. [CrossRef]

51. Porter, R.; Chen, K. Heat and mass transfer of sprays canals. *Heat Transf.* **1974**, *96*, 286–291. [CrossRef]

52. MATLAB-MathWorks-MATLAB & Simulink. Available online: https://uk.mathworks.com/products/matlab.html (accessed on 6 August 2020).

53. Thomas, B.; Murphy, D.J.; Murray, B.G. *Encyclopedia of Applied Plant Sciences*; Elsevier Ltd.: Amsterdam, The Netherlands, 2017; ISBN 978-0-12-394808-3.

54. Fritz, B.K.; Hoffmann, W.C.; Czaczyk, Z.; Bagley, W.; Kruger, G.; Henry, R. Measurement and classification methods using the ASAE S572.1 reference nozzles. *J. Plant Prot. Res.* **2012**, *52*, 447–457. [CrossRef]

55. Nuyttens, D.; de Schampheleire, M.; Steurbaut, W.; Baetens, K.; Verboven, P.; Nicolaï, B.; Ramon, H.; Sonck, B. Characterization of agricultural sprays using laser techniques. *Asp. Appl. Biol.* **2006**, *77*, 1–8.

56. Kabeel, A.E.; Bassuoni, M.M. A simplified experimentally tested theoretical model to reduce water consumption of a direct evaporative cooler for dry climates. *Int. J. Refrig.* **2017**, *82*, 487–494. [CrossRef]

57. Rezaei, E.; Shafiei, S.; Abdollahnezhad, A. Reducing water consumption of an industrial plant cooling unit using hybrid cooling tower. *Energy Convers. Manag.* **2010**, *51*, 311–319. [CrossRef]

58. Pontes, R.F.F.; Yamauchi, W.M.; Silva, E.K.G. Analysis of the effect of seasonal climate changes on cooling tower efficiency, and strategies for reducing cooling tower power consumption. *Appl. Therm. Eng.* **2019**, *161*, 114148. [CrossRef]